Physica A 410 (2014) 319–326

Contents lists available at ScienceDirect

Physica A

journal homepage: www.elsevier.com/locate/physa

Asymmetric Brownian transport in a family of corrugated two-dimensional channels

J. Alvarez-Ramirez *, L. Dagdug, L. Inzunza

División de Ciencias Básicas e Ingeniería, Universidad Autónoma Metropolitana-Iztapalapa, Apartado Postal 55-534, México D.F., 09340, Mexico

HIGHLIGHTS

- Brownian transport in corrugated channels is studied.
- Curved midline has the effect of entropic barrier.
- Axial asymmetry induces asymmetric directional transport.

ARTICLE INFO

Article history:
Received 13 November 2013
Received in revised form 10 April 2014
Available online 21 May 2014

Keywords:
Diffusion
Sinusoidal channel
Curved midline
Asymmetric transport

ABSTRACT

Brownian dynamics simulations of passive particles along two-dimensional channels with curved midline and varying width are considered in this work. By considering finite-length channels formed by sinusoidal unit cells, it was found that axial asymmetry (e.g., non-zero midline) can induce asymmetric particle transport in the sense that the particle current is dependent on the transport direction (either left-to-right or right-to-left). Geometrically, this is caused by a combination of transient transport mechanism and non-uniform variation of the channel width, which produces the effect of a conical, diverging or converging, tube. Numerical results and theoretical predictions show that sinusoidal channels with curved midline and varying width can exhibit important levels of current asymmetry. In this way, this class of channels can be used as mass transport rectifiers where Brownian particles move preferentially in one direction than in the opposite direction. It is also shown that the transport asymmetry vanishes as the particle trajectories approach equilibrium conditions for sufficiently large channels.

1. Introduction

The problem of diffusion in geometrically confined system arises in different contexts. Examples include transport of particles in biological cells and membranes [1,2] and in zeolites [3], catalytic reactions occurring on templates or in porous media [4], separation techniques of size disperse particles on micro-scales and nano-scales [5], controlled particle release [6,7] and many more. As pointed out by Burada et al. [8], the characterization of these transport phenomena involves studying geometrically constrained Brownian dynamics [9–11]. A close understanding of the phenomena underlying transport in confined geometries should allow accurate manipulation and design of structures oriented for controlling diffusion in, e.g., drug release and migration of contaminants in porous media.

Narrow corrugated channels belong to a class of geometries for confined transport of small particles (e.g., biomolecules and colloids) with application to both natural [1,3] and artificial devices [9]. These types of confinements are typically

* Corresponding author. Tel.: +52 5558044934.
E-mail address: jjar@xanum.uam.mx (J. Alvarez-Ramirez).

http://dx.doi.org/10.1016/j.physa.2014.05.054
0378-4371/

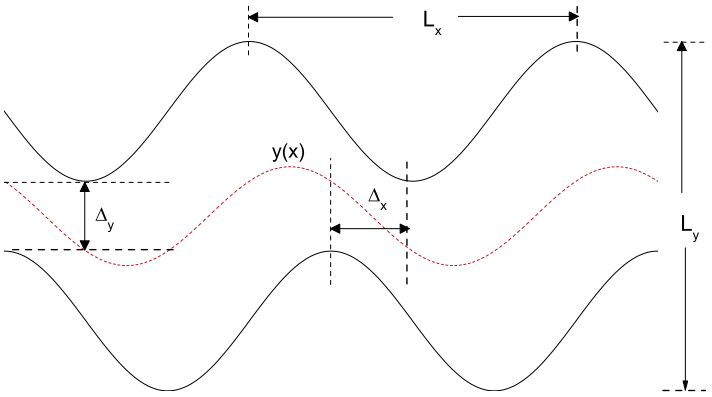

Fig. 1. Schematic diagram of shifted sinusoidal channels with vertical shift, Δ_y, and horizontal shift, Δ_x.

modeled as periodic channels with axial symmetry and unit cells delimited by bottlenecks [10]. It has been shown that, under certain restrictive conditions, narrow corrugated channels with smooth delimiting walls can be reduced to quasi-one-dimensional channels [11–14]. The main restriction for reducing the transport behavior into a one-dimensional channel is that the width rate of change be sufficiently small. However, recent technological developments have allowed the fabrication of channels with prescribed configurations. In many cases, the assumption of sufficiently small width rate of change is no longer satisfied. Motivated by this, diverse theoretical and numerical results have reported the transport characteristics of a large variety of narrow channel configurations. Rectification capabilities of corrugated channels have been also explored in Ref. [15,16], showing that a mesoscopic description of the transport phenomena can require some generalizations of Fick's law for accounting for apparent drift in diffusion gradient.

Of particular interest in recent years are narrow channels with curved midline and varying width, which contain axial asymmetries. Only a limited number of both theoretical and numerical results are available in the literature. Theoretical estimations of the effective diffusivity were recently reported [17–19] and the range of applicability of such estimations was numerically evaluated [20]. The effect of non-symmetric external forces in the particle current along the axial coordinate was recently evaluated [21].

This work considers Brownian particle transport in two-dimensional periodic narrow channels with curved midline and varying width. By using sinusoidal geometry for the limiting channel walls, numerical simulations of the Langevin equation revealed an interesting feature of this type of channels formed by a finite number of unit cells; namely, the emergence of asymmetric axial transport. That is, for certain channel configurations, Brownian particles are preferentially transported in one axial direction (e.g., left-to-right) than in the opposite axial direction. Numerical results and theoretical predictions show that the transport asymmetry can be explained from the combination of transient transport mechanisms and asymmetric channel geometry.

2. Model and methods

2.1. The family of corrugated two-dimensional channels

We consider overdamped Brownian particles moving in a periodic 2D channel, of unitary period, with the curved midline and narrow varying width, as shown in Fig. 1. Upper and lower walls are modeled by the sinusoidal functions $f_{up}(x)$ and $f_{low}(x)$, where

$$f_{up}(x) = \frac{1}{4}\left[\left(L_y + \Delta_y\right) - \left(L_y - \Delta_y\right)\cos\left(\frac{2\pi\,(x - \Delta_x)}{L_x}\right)\right] \tag{1a}$$

$$f_{low}(x) = -\frac{1}{4}\left[\left(L_y + \Delta_y\right) - \left(L_y - \Delta_y\right)\cos\left(\frac{2\pi x}{L_x}\right)\right]. \tag{1b}$$

Here, Δ_x and Δ_y correspond to the horizontal shift between the periodic walls and to the minimum wall distance, respectively. The channel width is given by $w(x) = f_{up}(x) - f_{low}(x)$, while the channel midline height is given by $h(x) = \frac{1}{2}\left[f_{up}(x) + f_{low}(x)\right]$. It is noted that $h(x) \to 0$ as $\Delta_x \to 0$, which corresponds to a vertically symmetrical channel. The variation of the parameter Δ_x in the range $[0, 0.5]$ leads to a series of serpentine-like channels with curved midline and varying width, as shown in Fig. 2. For Δ_x in the range $[0.5, 1.0]$, the resulting channels correspond to the mirror reflection of that for the range $[0, 0.5]$. In this way, it suffices to consider the series of channels obtained within the horizontal shift range $[0, 0.5]$.

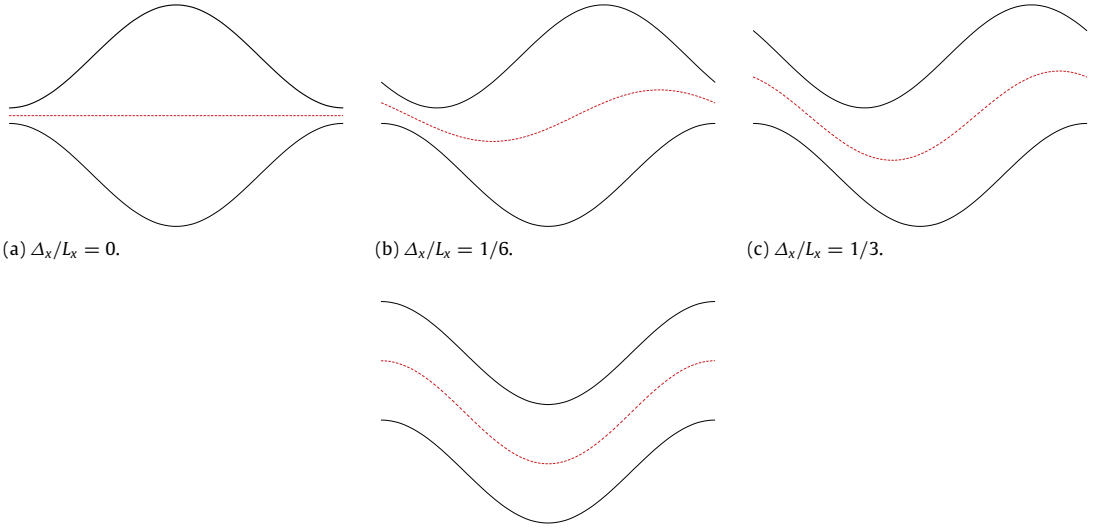

(a) $\Delta_x/L_x = 0$. (b) $\Delta_x/L_x = 1/6$. (c) $\Delta_x/L_x = 1/3$.

(d) $\Delta_x/L_x = 1/2$.

Fig. 2. Geometry of sinusoidal channels for different horizontal shifts, Δ_x/L_x.

2.2. Numerical simulations

The overdamped dynamics of the particle is modeled by the 2D Langevin equation

$$\frac{d\mathbf{r}}{dt} = \sqrt{2D_0}\boldsymbol{\xi}(t) \tag{2}$$

where $\mathbf{r} = (x, y)$ is the coordinates vector. Here, $\xi(t) = (\xi_x(t), \xi_y(t))$ are zero-mean white Gaussian noises with autocorrelation functions $\langle \xi_i(t), \xi_j(t') \rangle = \delta_{ij}\delta(t - t')$ with $i, j = x, y$. Eq. (2) was numerically integrated by using a Milstein algorithm [22]. Stochastic averages were obtained as ensemble averages over 10^5 trajectories. Transient effects were estimated and subtracted.

For fixed parameters Δ_y, L_x and L_y, one is interested in evaluating the effects of non-zero midline (i.e., Δ_x) in the transport of Brownian particles along the horizontal x-direction. Relative to the horizontal shift Δ_x, the channel geometry is periodic with unit period. Also, the channel geometry is anti-symmetric with respect to the center value $\Delta_x/L_x = 0.5$. In this way, it suffices to consider channels with horizontal shift within the range $\Delta_x/L_x = [0, 0.5]$. To quantify the channel transport properties, the time required for a particle for horizontally crossing the channel from a boundary to the other is considered. The first passage time, denoted by T_{FPT}, is computed by placing the particle in either the left or right boundary and allowing the particle to move for reaching the opposite boundary by first time. In this way, initial conditions are randomly distributed in either the left ($x = 0$) or the right ($x = L_x$) boundary. Also, the initial position serves as the reflecting boundary. For each particle, the time for numerical integration is finished when the particle crosses the exit boundary at $x = L_x$. The first passage time T_{FPT} is taken as the time for a particle to move from the entrance to the exit of the channel. As mentioned above, the mean first passage time (MFPT), denoted by $T_{MFPT} = \langle T_{FPT} \rangle$, is computed over 10^5 trajectories. It is noted that the inverse of the average first passage time, $J = \frac{1}{T_{MFPT}}$, is an index of the particles current (i.e., flux) of particles along the channel.

2.3. Theoretical predictions

For an arbitrary channel, Kalinay [23] derived the following equation for predicting the MFPT along the axial direction:

$$T_{MFPT} = \int_0^{L_x} \frac{\Omega(x)}{w(x)D_{eff}(x)} dx \tag{3}$$

where $D_{eff}(x)$ is the position-dependent effective diffusivity, $w(x)$ is the channel width and $\Omega(x) = \int_0^x w(x')dx'$. Eq. (3) will be used for obtaining theoretical predictions of the MFPT and making a comparison with the numerical results from the simulations of the Langevin equation (2). To this end, a suitable expression for the effective diffusivity $D_{eff}(x)$ is required. For channels with zero midline, one can use the following equation proposed by Reguera and Rubi [13]:

$$D_{eff}(x) = \frac{D_0}{\left(1 + \frac{w'(x)^2}{4}\right)^{1/3}} \tag{4}$$

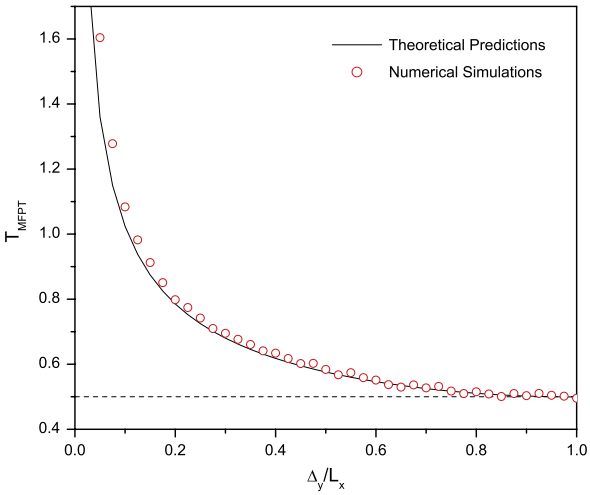

Fig. 3. Comparison between the MFPT estimated by numerical simulations of the Langevin equation and the theoretical prediction given by Eq. (3).

where $w'(x)$ is the derivative of the channel width. The curved midline has an important effect in the transport of Brownian particles along the axial direction. It is noted that Eq. (4) does not take into account this effect. Recently, Dagdug and Pineda [18] used projection methods for deriving the following effective diffusivity equation for channels with curved midline and varying width:

$$D_{eff}(x) = \left[\frac{\arctan\left(y_0'(x) + \frac{w'(x)}{2}\right)}{w'(x)} - \frac{\arctan\left(y_0'(x) - \frac{w'(x)}{2}\right)}{w'(x)} \right] D_0 \tag{5}$$

where $y_0'(x)$ is the derivative of the channel midline. In this way, Eq. (5) can be used in Eq. (3) for obtaining a theoretical estimation of the MFPT. To this end, it should be recalled that $w(x) = f_{up}(x) - f_{low}(x)$ and $y_0(x) = \left(f_{up}(x) + f_{low}(x)\right)/2$. The integrals involved in Eq. (3) were numerically solved by means of Simpson's Rule for numerical integration.

3. Results and discussion

In the sequel, without loss of generality, unitary length (i.e., $L_x = L_y = 1$) will be used with an integration step of 10^{-5} time units. As a preliminary step for assessing the effects of axial asymmetry in diffusion transport, the stability of the numerical scheme for the simulation of the Langevin equation (2) was evaluated against the theoretical predictions given by Eq. (3) for channels with zero midline (i.e., $\Delta_x = 0$). Here, $w(x) = \frac{1}{2}\left[\left(L_y + \Delta_y\right) - \left(L_y - \Delta_y\right)\cos\left(\frac{2\pi x}{L_x}\right)\right]$ and the position-dependent effective diffusivity $D_{eff}(x)$ is given by Eq. (4). Fig. 3 presents the MFPT as a function of the normalized vertical shift Δ_y/L_x. Good agreement between the results obtained from Eq. (3) and the Brownian dynamics simulation can be observed. As the channel width is increased, Brownian particles find fewer channel obstructions for moving freely before hitting the exit boundary. In this way, as shown in Fig. 3, the MFPT decreases monotonously with the vertical shift. The accuracy of the Brownian dynamics simulation can be also checked against the theoretical asymptotic value for a channel without obstructions. In such case, the MFPT can be obtained from Eq. (3) with $w(x) = \text{constant}$ and $D(x) = D_0$, giving $\frac{L_x^2}{2D_0} = 0.5$. It is noted that both the Brownian dynamics simulation and the theoretical prediction converge asymptotically to the expected value of 0.5.

3.1. Transport asymmetry in channels with curved midline and varying width

Fig. 2(a) and (d) indicate that the channels with horizontal shifts $\Delta_x/L_x = 0.0$ and $\Delta_x/L_x = 0.5$ are axially symmetric. That is, the channel first-half is the mirror image of the channel second-half. As a consequence, the estimation of the average first passage time T_{MFPT} is not dependent of the boundary at which particle trajectory is initiated. However, it is apparent that this is not the case for the non-extreme shifts $\Delta_x/L_x \in (0.0, 0.5)$. For vertical shift $\Delta_y/L_x = 0.05$, Fig. 4(a) presents the variation of the channel width $w(x)$ for four different values of the horizontal shift Δ_x/L_x. As expected, $w(x)$ is a symmetrical function with respect to the channel midpoint $x/L_x = 0.5$. However, the asymmetry is broken for the other cases. To quantify the asymmetry, the average channel width for the first ($0.0 \leq x/L_x \leq 0.5$) and second ($0.5 \leq x/L_x \leq 1.0$) horizontal channel halves was computed. Also for $\Delta_y/L_x = 0.05$, Fig. 4(b) exhibits the average widths as functions of the horizontal shift Δ_x/L_x. The difference between the first- and second-half average widths can be considered as an index of the channel asymmetry.

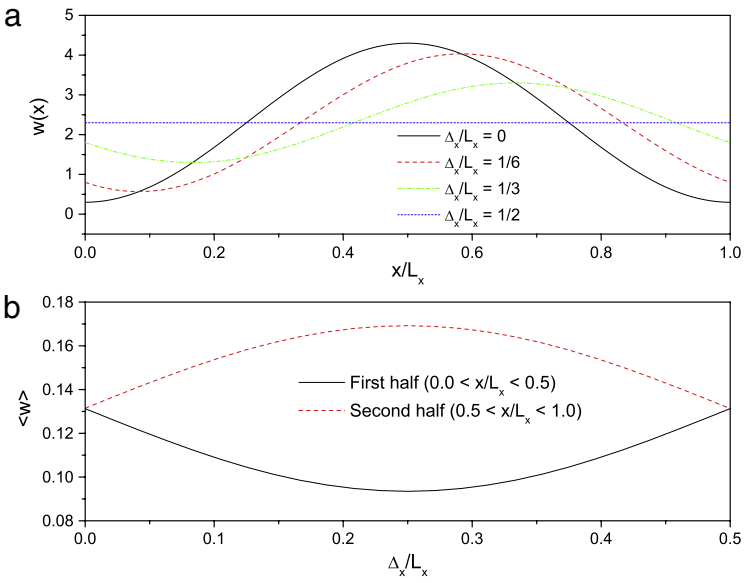

Fig. 4. (a) Channel width as a function of the horizontal x-coordinate, for vertical shift $\Delta_y/L_x = 0.05$. (b) First-half and second-half average widths as functions of the horizontal shift Δ_x/L_x. Maximum difference is found for $\Delta_x/L_x = 0.25$.

In this way, the channel asymmetry is zero for $\Delta_x/L_x = 0.0$ and $\Delta_x/L_x = 0.5$, and increases as the horizontal shift departs from these values. The maximum asymmetry is found for $\Delta_x/L_x \approx 0.25$.

Fig. 4(b) shows that the first-half mean width is smaller than the corresponding second-half mean width. In this way, the channel geometry resembles that of a conic channel with divergent width [24]. The conic channel is asymmetric in the x-coordinate, and it was found that such axial asymmetry induces transport asymmetries in the particle diffusion properties in the longitudinal direction. In fact, numerical results indicated that the effective diffusion along the width diverging direction is smaller than in the width converging direction. The results in Fig. 4(b) suggest that asymmetric transport can be exhibited by the sinusoidal channels. In this way, it is expected that particles are easier transported for the left-to-right (LR) than for the right-to-left (RL) direction. For evaluating the transport asymmetry, the mean first passage time was estimated and, for gaining physical insight, the results are presented in terms of the particle current $J = \frac{1}{T_{MFPT}}$. For three different values of the vertical shift Δ_y/L_x, Figs. 5 and 6 present the numerical results from simulations of Eq. (2) and the theoretical predictions from Eq. (3). The theoretical MFPT in the RL direction was computed by the direct application of Eqs. (3) and (5): for the MFPT in the LR direction, Eq. (2.18) from Ref. [23] has to be solved with the exchanged left and right boundary conditions, which is equivalent to using the horizontal coordinate change $x \mapsto L_x - x$. The results obtained from numerical simulations (symbols labeled as NS) and theoretical predictions (lines labeled as TP) are exhibited in Figs. 5 and 6. In this regard, the following comments are in order:

(a) For three different values of the vertical shift Δ_y/L_x, the particles currents in the LR and RL directions are exhibited in Fig. 5 as functions of the horizontal shift Δ_x/L_x. It is noted that the directional currents are not monotonous functions, but exhibit a minimum and a maximum for the LF and the RL directions, respectively. This means that the larger obstruction (facilitation) for the Brownian transport is not found for the symmetric and the fully asymmetric cases. In fact, the larger transport obstruction (facilitation) is found for a horizontal shift somewhere between the symmetric and the fully asymmetric cases. As expected, higher particle currents are obtained for LR than for the RL direction, confirming that the horizontally shifted channels induce asymmetric Brownian transport.

(b) It can be observed that the current is an increasing function of the vertical shift Δ_y/L_x. When $\Delta_y/L_x \to 0$ and $\Delta_x/L_x \to 0$, the channel becomes blocked and particles cannot pass from one boundary to another, so the particle current J is zero. However, horizontal shifts remove the channel blocking, allowing the movement of particles along the channel cells. On the other hand, when $\Delta_y/L_x \to \infty$, the channel approaches a configuration with zero midline and the effect of the corrugation disappears. In such case, the particle motion behaves as that of particles in unconstrained geometries. Although the theoretical predictions, represented by the lines in Fig. 5, exhibit a shape similar to that obtained with numerical simulations, important deviations can be observed. The differences between numerical simulations and theoretical prediction can be due to the fact that the effective diffusivity equation (5) was derived by assuming equilibrium conditions (i.e., for large times) [18], while the transport across the channels is achieved in finite times. In this way, Eq. (5) provides poor estimates of the position-dependent diffusivity for large derivatives of the channel midline.

(c) Fig. 6(a) presents the net particles current in the channel, which is defined as $\frac{J_{RL}+J_{LR}}{2}$. In contrast to the directional currents, the net particles current exhibits a non-monotonous increasing behavior with respect to the horizontal shift

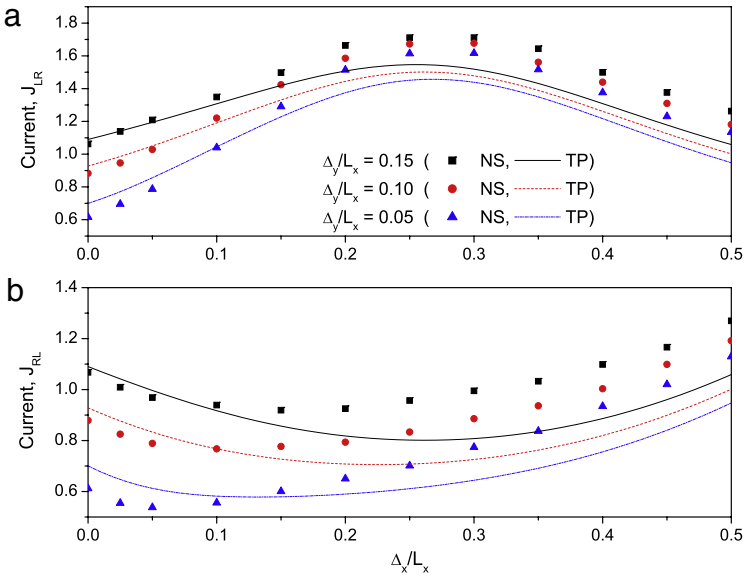

Fig. 5. Directional (either left-to-right or right-to-left) particle current, J, across a unit cell, as a function of the horizontal shift, Δ_x/L_x. Important differences in the directional transport are displayed. Numerical simulations (NS) are represented by symbols, while theoretical predictions (TP) by lines.

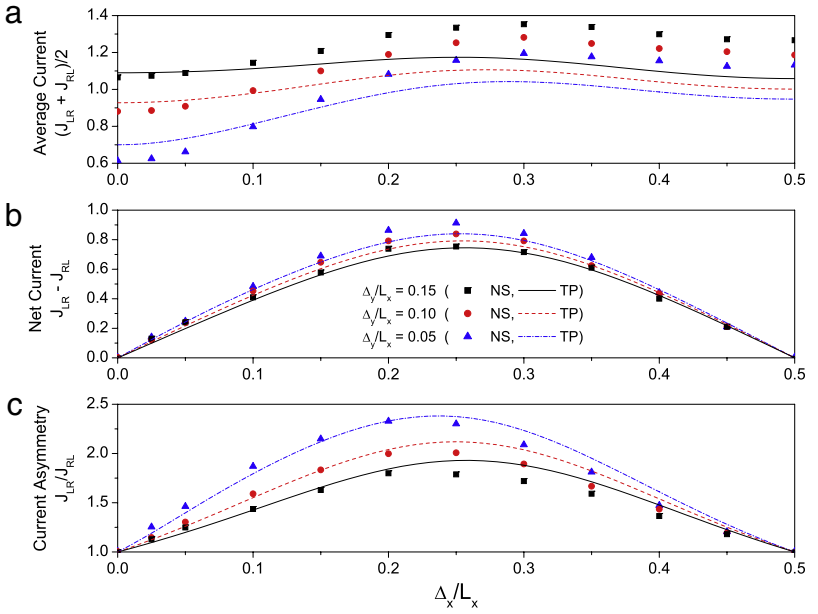

Fig. 6. (a) Non-directional particle current across a unit cell, as a function of the horizontal shift Δ_x/L_x. (b) Net particle current quantified as the difference in either directions. (c) Transport asymmetry quantified as the ratio of currents between left-to-right and right-to-left transport. Numerical simulations (NS) are represented by symbols, while theoretical predictions (TP) by lines.

Δ_x/L_x. The lower and higher non-directional currents are found for $\Delta_x/L_x = 0.0$ and $\Delta_x/L_x \approx 0.3$, respectively. In turn, such a behavior indicates that the better conditions for Brownian particle transport are exhibited by serpentine-like channels for which the width is nearly constant. In contrast, channels with $\Delta_x/L_x = 0.0$ exhibit a compartment-like geometry with bottleneck that limits the effective velocity at which particles are transported. Interestingly, theoretical predictions show good agreement with numerical results only for relatively small values of the horizontal shift Δ_x/L_x, corresponding to small deviations from a channel configuration with zero midline.

(d) The net particle current across the unit cell can be defined as $|J_{RL} - J_{LR}|$, indicating the current difference across the channel. The results are presented in Fig. 6(b), showing that the higher net current is achieved for horizontal shift $\Delta_x/L_x \approx 0.25$. That is, particles tend to move preferentially in one direction than in the other. In contrast to the directional currents (Fig. 5) and the net current (Fig. 6(a)), the theoretical predictions are in good agreement with

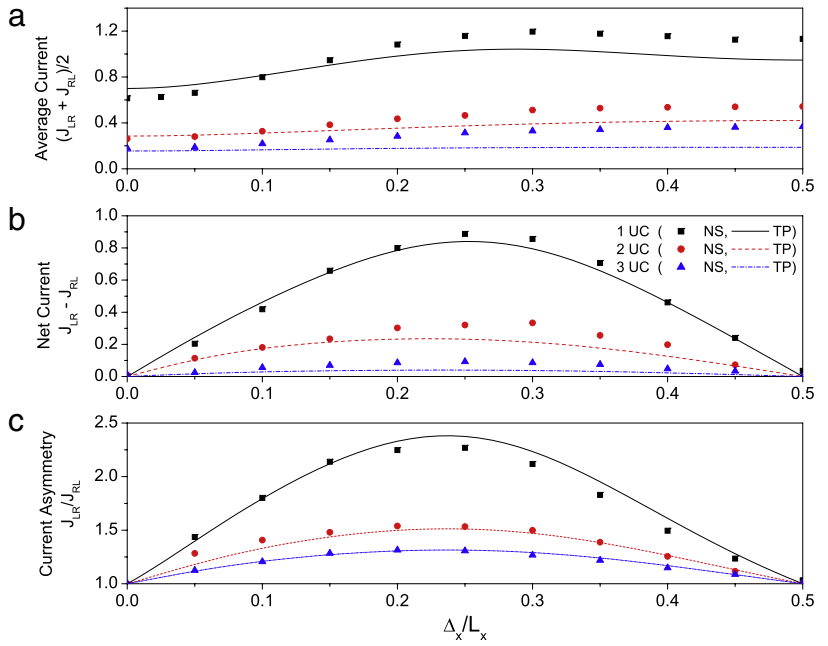

Fig. 7. Transport results for channels with vertical shift $\Delta_y/L_x = 0.05$ and three different numbers of unit cells (UC). Numerical simulations (NS) are represented by symbols, while theoretical predictions (TP) by lines. (a) Non-directional particle current for one, two and three unit cells. (b) Net particle current quantified as the difference in either directions. (c) Transport asymmetry quantified as the ratio of currents between left-to-right and right-to-left transport.

numerical simulations. This improved agreement can be caused by a sort of compensation effect between the LR and RL directional currents. It is apparent that the finite-time effects in either direction are partially compensated by the finite-time effects in the opposite direction.

(e) Fig. 4(b) showed that the higher width asymmetry is displayed for horizontal shift $\Delta_x/L_x \approx 0.25$. This feature should be reflected in the transport properties. The current ratio $\frac{J_{LR}}{J_{RL}}$ can be used as an index for quantifying the transport asymmetry, and the results are shown in Fig. 6(c). In line with the width asymmetry, the numerical results show that the maximum transport asymmetry is found for $\Delta_x/L_x \approx 0.25$. In this way, the sinusoidal channel with horizontal shift $\Delta_x/L_x \approx 0.25$ can be used as a mass transport rectifier where Brownian particles move preferentially in the direction of increasing width than in the direction of decreasing width. It is noted that Eqs. (3) and (5) offer accurate predictions of the transport asymmetry only for relatively small values of the horizontal shift Δ_x/L_x, when channels exhibit small deviations from the zero midline configuration. This suggests that Eq. (5) provides inaccurate effective diffusivity predictions for channels with large midline derivative $y_0'(x)$.

3.2. Effect of the number of unit cells

It should be remarked that the results described in Fig. 6 were obtained for a unit cell of finite length where equilibrium Brownian transport is hardly achieved. In this way, the transport asymmetry is induced by transient mechanisms in combination with asymmetries of the channel geometry. For long random walk times, equilibrium is approached and the transport asymmetries should be diminished. At equilibrium conditions, the directional transport difference must be vanished. In geometric terms, random walk equilibrium conditions can be approached when the Brownian particles move in an infinite series of unit cells. For $\Delta_y/L_x = 0.05$, Fig. 7 presents the numerical simulation results for finite-length channels with one, two and three unit cells. For a fair comparison between channels with different number of unit cells, the particle current is normalized as $J = \frac{N_C}{T_{MFPT}}$, where N_C is the number of unit cells. It is apparent that the current asymmetry decreases monotonously with the number of unit cells in the transport channel. Dynamically, the reduction of the current asymmetry is caused by a mixing phenomenon where particles can go back and forth between unit cells. In the limit of a large number of unit cells, the particle trajectories are well mixed, leading to a vanishing of the transport asymmetry. The theoretical predictions given by Eqs. (3) and (5) were improved for increasing number of unit cells. This is not a surprising result at all, since increasing the number of unit cells reduces the transient effects of the Brownian trajectories, improving in this way the predictions of the effective diffusivity equation (5) [18]. In principle, for sufficiently large channels (i.e., for a very large number of unit cells), the Brownian trajectories should attain equilibrium conditions and Eq. (5) should provide an accurate prediction of the effective-diffusivity. However, as illustrated in Fig. 7(c), the transport asymmetry tends to zero for sufficiently large channels, regardless of the curved midline.

4. Concluding remarks

This work studied the transport of overdamped Brownian particles in two-dimensional corrugated channels with curved midline and narrow varying width. By considering channels formed by unit cells, it was shown that the varying width can introduce axial asymmetries, which in turn lead to asymmetric transport. The higher symmetric transport is found for the midterm between a symmetrical channel configuration and a serpentine-like channel with constant width. Also, the transport asymmetry is reduced with increasing number of unit cells since particle trajectories tend to achieve equilibrium conditions. The results obtained in this work show that asymmetries can be advantageously considered for application in many processes, such as transport in meso- and nano-structured membranes, controlled drug release and rectification of particle transport in corrugated channels. In fact, recent advances in the development of meso- and nano-structured materials allow the fabrication of channels with prescribed geometries, as those studied in this work.

Finally, the transport asymmetry reported in our work is similar in nature to that reported in Ref. [24]. Namely, transport asymmetry, reflected as differences in the directional MFPT, can be explained from differences in the channel width derivative in the LR and RL directions. The simplest case is the conic channel with constant midline explored in the aforementioned paper. The channels described in Fig. 2 can be seen as topologically equivalent to piecewise compositions of conic channels to yield non-centered midline. The main difference with the asymmetric transport results for conic channels is that the curved midline and the varying width magnify the asymmetry of the MFPT.

References

[1] B. Hille, Ion Channels in Excitable Membranes, Sinauer Associates, Sunderland, MA, 2001.
[2] B. Alberts, A. Johnson, J. Lewis, M. Raff, K. Roberts, P. Walter, Molecular Biology of the Cell, Garland, New York, 2007.
[3] J. Karger, D.M. Ruthven, Diffusion in Zeolites and Other Microporous Solids, Wiley, New York, 1992.
[4] M.C. Daniel, D. Astruc, Chem. Rev. 104 (1997) 293.
[5] A. Corma, Chem. Rev. 97 (1997) 2373.
[6] N.F. Sheppard, D.J. Mears, S.W. Straks, J. Controlled Release 42 (1996) 15.
[7] J.T. Santini Jr., M.J. Cima, R. Langer, Nature 397 (1999) 335.
[8] P.S. Burada, P. Hänggi, F. Marchesoni, G. Schmid, P. Talkner, ChemPhysChem. 10 (1997) 45.
[9] P. Hanggi, F. Marchesoni, Rev. Modern Phys. 81 (2009) 387.
[10] P.K. Ghosh, P. Hanggi, F. Marchesoni, F. Nori, G. Schmid, Phys. Rev. E 86 (2012) 021112.
[11] R. Zwanzig, J. Phys. Chem. 96 (1992) 3296.
[12] P. Kalinay, J.K. Percus, Phys. Rev. E 74 (2006) 041203.
[13] D. Reguera, J.M. Rubi, Phys. Rev. E 64 (2001) 061106.
[14] D. Reguera, G. Schmid, P.S. Burada, J.M. Rubi, P. Reimann, P. Hanggi, Phys. Rev. Lett. 96 (2006) 130603.
[15] F. Marchesoni, S. Savel'ev, Phys. Rev. E 80 (2009) 011120.
[16] F. Marchesoni, Materials 6 (2013) 3598–3609.
[17] R.M. Bradley, Phys. Rev. E. 80 (2009) 061142.
[18] L. Dagdug, I. Pineda, J. Chem. Phys. 137 (2012) 024107.
[19] S. Martens, I.M. Sokolov, L. Schmansky-Geier, J. Chem. Phys. 137 (2012) 174103.
[20] I. Pineda, J. Alvarez-Ramirez, L. Dagdug, J. Chem. Phys. 137 (2012) 174103.
[21] F. Li, B. Ai, Phys. Rev. E 87 (2013) 062128.
[22] P. Kloeden, E. Platen, Numerical Solutions of Stochastic Differential Equations, Springer, Berlin, 1999.
[23] P. Kalinay, J. Chem. Phys. 126 (2007) 194708.
[24] A.M. Berezhkovskii, M.A. Pustovoit, S.M. Bezrukov, J. Chem. Phys. 126 (2007) 134706.